

GPU-based Graph Traversal on Compressed Graphs

Mo Sha

School of Computing
National University of Singapore
sham@comp.nus.edu.sg

Yuchen Li

School of Information System
Singapore Management University
yuchenli@smu.edu.sg

Kian-Lee Tan

School of Computing
National University of Singapore
tankl@comp.nus.edu.sg

ABSTRACT

Graph processing on GPUs received much attention in the industry and the academia recently, as the hardware accelerator offers attractive potential for performance boost. However, the high-bandwidth device memory on GPUs has limited capacity that constrains the size of the graph to be loaded on chip. In this paper, we introduce GPU-based graph traversal on compressed graphs, so as to enable the processing of graphs having a larger size than the device memory. Designed towards GPU's SIMT architecture, we propose two novel parallel scheduling strategies *Two-Phase Traversal* and *Task-Stealing* to handle thread divergence and workload imbalance issues when decoding the compressed graph. We further optimize our solution against power-law graphs by proposing *Warp-centric Decoding* and *Residual Segmentation* to facilitate parallelism on processing skewed out-degree distribution. Extensive experiments show that with 2x-18x compression rate, our proposed GPU-based graph traversal on compressed graphs (GCGT) achieves competitive efficiency compared with the state-of-the-art graph traversal approaches on non-compressed graphs.

ACM Reference Format:

Mo Sha, Yuchen Li, and Kian-Lee Tan. 2019. GPU-based Graph Traversal on Compressed Graphs. In *2019 International Conference on Management of Data (SIGMOD '19), June 30–July 5, 2019, Amsterdam, Netherlands*. ACM, New York, NY, USA, 18 pages.
<https://doi.org/10.1145/3299869.3319871>

1 INTRODUCTION

Graph analysis is a powerful tool to unveil hidden patterns and knowledge from complex data with a sparse schema. To meet the demand for analyzing large-scale graphs emerging from a wide range of applications, e.g., social networks, web

graphs, transaction networks and many others, there is a prevailing interest in developing parallel algorithms to empower efficient or even real-time graph analysis [18, 25, 47, 51]. Meanwhile, the exceptional advances of General-Purpose GPUs (GPGPUs) have completely revolutionized the computing paradigm across multiple fields [34]. Massive number of cores and ultra memory bandwidth make GPUs a promising platform for accelerating graph processing. Existing efforts have shown great success in parallelizing graph algorithms on GPUs, such as BFS [30, 33, 46], PageRank [15, 37, 49], Connected Component [2, 42], Betweenness Centrality [44], Graph Label Propagation [43], etc.

The acceleration enabled by GPUs, however, does not come for free. When the graph size exceeds the GPU device memory, costly data transfer between CPUs and GPUs is inevitable. Unlike the RAM architecture, the device memory is fixed in the printed circuit board (PCB) and cannot be extended. The memory size of mainstream GPUs is typically at most 12 GB, which translates to storing graphs with two billion edges at best. There have been several strategies proposed to support processing graphs with a size larger than the device memory: the out-of-core strategy [26, 36, 39] that divides data into tiles and overlaps the data transfer with GPU computation to hide the communication overhead, the multi-GPU strategy [3, 32, 35, 50] as well as the distributed GPU cluster strategy [17, 21, 46]. In this paper, we propose an orthogonal approach to further expand the capability of GPU graph processing. The high level idea is rather intuitive: we execute the GPU workloads on a compressed graph and only decode necessary data into caches to limit the memory usage. Since graph processing tasks are mostly bounded by memory accesses, we leverage on the massive computing power of GPUs to hide the decoding cost and retain the performance as that in the uncompressed scenario. Given that the market price of GPU device with a large memory size is expensive, e.g., GV100 with 32GB device memory costs \$9,000 per device, our proposed approach reduces the pressure of memory usage for single-GPU environment. The benefits carry over when one resorts to the multi-GPU environment or the distributed environment.

However, this seemingly intuitive idea brings non-trivial technical challenges. The key strategy of processing graphs on GPUs is to evenly distribute the neighbor nodes of an adjacency list into balanced workloads assigned to multiple

Permission to make digital or hard copies of all or part of this work for personal or classroom use is granted without fee provided that copies are not made or distributed for profit or commercial advantage and that copies bear this notice and the full citation on the first page. Copyrights for components of this work owned by others than the author(s) must be honored. Abstracting with credit is permitted. To copy otherwise, to republish, to post on servers or to redistribute to lists, requires prior specific permission and/or a fee. Request permissions from permissions@acm.org.
SIGMOD '19, June 30–July 5, 2019, Amsterdam, Netherlands
© 2019 Copyright held by the owner/author(s).
Publication rights licensed to ACM.
ACM ISBN 978-1-4503-5643-5/19/06...\$15.00
<https://doi.org/10.1145/3299869.3319871>

threads. This does not hold if graphs are stored in a compressed manner, since the threads are unable to identify the neighbor nodes from their compressed form directly. This is rather challenging for scheduling GPUs' workloads for three major reasons. First, it is difficult to estimate the workload in advance for assigning threads in a balanced manner, in contrast to processing uncompressed graphs. Second, it is challenging to dynamically reschedule the workload for massive GPU threads as compared to the CPU environment since each single processing unit of GPUs contains minimum number of control units and is far less powerful as compared to one CPU core. Third, we need to bound the decoding process within GPU's cache to ensure that the performance does not degrade compared with the uncompressed scenario, as decoding into global memory is prohibitively expensive. To address the aforementioned challenges, we propose GPU-based Compressed Graph Traversal (GCGT), an *in-cache* scheme to traverse the compressed graph representation (CGR) stored in GPU's device memory.

A direct parallel approach assigns a thread to decode a compressed adjacency list. However, such direct approach renders severe thread divergence issue since concurrent threads may end up in diverging control branches when decoding different segments of the compressed adjacency lists. Thus, we propose GPU-oriented scheduling strategies under GCGT: *Two-Phase Traversal* and *Task-Stealing*. *Two-Phase Traversal* explicitly synchronizes thread groups and ensures the threads entering the same control branch while decoding their respective adjacency lists. When a few threads are heavily loaded, we employ *Task-Stealing*: the working threads push their extra workload to the shared memory and the idle threads then steal the workload for better GPU utilization. Furthermore, we observe that the skewed distribution of power-law graphs leads to the workload imbalance problem and our proposed scheduling strategies only achieve sub-optimal results as they are structure-transparent. To support power-law graphs, we first propose a novel *Warp-centric Decoding* to effectively parallelize the decoding process. Second, we partition long adjacency lists into segments and devise a *Residual Segmentation* strategy for threads to better collaborate under GCGT. To the best of our knowledge, this is the first study on how to traverse compressed graphs of its kind on GPUs.

The contributions of this paper are summarized as follows:

- We introduce GCGT, a novel scheme to enable GPUs for traversing compressed graph representation (CGR) directly. We propose *Two-Phase Traversal* and *Task-Stealing* strategies to reduce thread divergence while decoding adjacency lists in parallel.
- We devise novel *Warp-centric Decoding* and *Residual Segmentation* optimizations to support efficient power-law graph processing under GCGT.

- We conduct an extensive experimental study on various types of graph datasets in different scales. The experimental results reveal that GCGT achieves 2x-18x compression rate while producing competitive efficiency against the state-of-the-art GPU graph traversal approaches.

The rest of this paper is organized as follows. In Section 2, we review existing related studies. Then in Section 3, we present the preliminaries. Section 4 demonstrates the proposed GPU-based compressed graph traversal algorithms and Section 5 discusses the optimizations for power-law graphs. We discuss how to extend GCGT to other graph applications in Section 6. Next, we present the experimental evaluation in Section 7 and finally, we conclude in Section 8.

2 RELATED WORK

We survey some related studies in this section. First, we discuss the literature on GPU-based graph processing. Then, we review existing methods for graph compression.

2.1 GPU-based Graph Processing

Emerging trends for GPU computing have influenced a wide range of data-intensive and compute-intensive tasks, including large-scale graph processing. There are a plethora of recent studies which focus on developing efficient parallel computational frameworks for graph processing on GPUs. Medusa [51] is the first framework to support general graph processing on GPUs. It provides a set of user-defined APIs, on top of which the users express their sequential programs and Medusa does the automatic scheduling on GPUs. CuSha [25] is a node-centric graph processing platform and is based on G-Shards, a static GPU-friendly graph data representation designed for higher memory access efficiency. GPMA [38] proposes a dynamic graph analytic framework on GPUs, where both graph updates and graph processing are efficiently supported. Gunrock [47] offers a higher-level abstraction than Medusa, which corresponds to an operation on the nodes or edges in graphs. These GPU-based graph processing frameworks make it simpler to program GPUs for general graph computation and at the same time, achieve superior speedups compared with the multi-core CPU systems.

In addition to the aforementioned general frameworks, a variety of typical graph problems have been investigated for GPU acceleration [2, 15, 20, 29, 37, 42, 43, 49]. In particular, Breath First Search (BFS) has been extensively studied lately [17, 30, 33, 46]. Parallelizing BFS-style graph traversal on GPUs mostly follows the *expansion - filtering - contraction* computational pipeline. To be specific, such graph computation is based on ping-pong frontier queues in an iterative manner. In each round, the out-degrees of frontiers in in-Queue are traversed, then filtered by application-specific requirements and finally placed into outQueue. In this work,

we propose GCGT to parallelize BFS traversal on compressed graph representations (CGR) stored in GPUs. GCGT is not limited to BFS since its computation pipeline generalizes to a wide range of parallel graph algorithms on GPUs, such as Connected Component [42], Betweenness Centrality [44], Personalized PageRank [20] and Label Propagation [43].

The main concern of processing BFS on GPU stems from irregular memory accesses. For one thing, frontiers to be handled in each iteration are generally distributed randomly, which leads to uncoalesced memory accesses. For another, the out-degrees of frontiers are skewed (in most real-world datasets, they follow the power-law distribution). This gives rise to thread divergence and results in degradation of the core utilization [45]. To alleviate these issues, existing studies rely on adaptively distributing the out-degrees of frontiers to thread groups of variable sizes [30, 33]. However, traversal on CGR incurs a greater challenge since the workloads cannot be easily estimated before decompression. One naïve solution decompresses the out-degrees of frontiers in the device memory and then employs existing optimizations to evenly distribute the workloads to threads. However, this trivial solution not only results in frequent device memory accesses at a high latency but also potentially takes $O(E)$ space, which defeats the purpose of utilizing CGR in the first place. Thus, different from this trivial solution, GCGT proposes a set of novel approaches to decompress and process frontier neighbors entirely in the GPU cache.

2.2 Graph Compression

Existing graph compression techniques can be broadly classified into two categories: (i) reduce the number of edges through introducing auxiliary structures; (ii) for a certain given edge list, use fewer bits in the representation. It is noted that the categories are orthogonal to each other and can be applied together.

Category (i). *Virtual Node Compression* [10] is one of the most popular graph compression approaches that introduce auxiliary structures. It searches for frequent patterns of nodes appearing in the adjacency lists and replaces them with virtual nodes. Such an approach can effectively reduce the number of edges and retain the equivalent graph topology. Virtual node compression attracts several follow-up studies on graph processing [11, 24] due to its good compatibility and proven effectiveness, especially on web graphs. Similarly, N. Larsson et al. propose Re-Pair [28], which replaces a frequent pair of symbols with a new symbol repeatedly as a grammar-compression approach. Based on this study, F. Claude et al. [13] introduce Re-Pair to the area of graph compression to reduce the number of stored edges.

Category (ii). Compressed graph representation (CGR) focuses on minimizing the number of bits required to represent

a graph. BV [7, 8] is a widely adopted technique to compress web graphs [31], and it supports general graph data as well. BV takes advantage of the similarity and locality in graph data, reuses the redundant information in the areas which are close to each other in the graph, and then records data via VLC in order to compress the bits per edge. In the meanwhile, a number of node reordering techniques have been proposed to achieve higher compression rate on top of the BV encoding scheme. Apostolico et al. [1] study the encoding and the compression of graphs based on node indices assigned by the BFS order. In Shingle [12], it is argued that the algorithm of finding the optimal encoding scheme so as to achieve the minimal bits per edge has a high complexity, and then an approximate optimization algorithm based on MinHash is proposed. Subsequently, in BP [14], an extension of Shingle, it is shown that finding the optimal encoding scheme is NP-hard and an improved, approximate optimization algorithm on the basis of recursive graph bisection is devised. Slash-Burn [23] removes the Hub nodes in the graph structure so that it can obtain an encoding scheme with better locality. Similarly, LLP [5] aims to obtain clusters with similarity in the graph structure in a layered label propagation manner. Furthermore, a fixed-length compression approach [22] is proposed to represent integers in a tight fixed-length manner. Specifically, it sets the length of integer as short as possible on the premise that the number of nodes in a graph does not overflow. However, its effectiveness is constrained by the range of the represented values, which renders the approach unable to scale to large graphs with millions of nodes.

Summary. Existing studies devise optimization specific to different types of graphs and achieve a satisfactory compression rate. The proposed GCGT is orthogonal to existing graph compression techniques since we focus on how to efficiently process graph traversals on the compressed format directly. In other words, existing compression techniques may serve as a preprocessing step for GCGT. Henceforth, we carefully examine the trade-off between the compression rate of existing work and the efficiency of our proposed techniques working with these compression schemes.

3 PRELIMINARIES

In this section, we start with introducing the background knowledge of CGR. Next, we present an overview of our GPU-based compressed graph traversal (GCGT). Readers can get more information on the computational architecture of GPUs in Appendix A.

3.1 Compressed Graph Format on GPUs

Given a graph $G = (V, E)$ (either directed or undirected), V is the node set and E is the edge set. Let $\text{OutDeg}(u) = \{v \in V | (u, v) \in E\}$ denote node u 's out-degree in G . In graph applications, Compressed Sparse Row (CSR) is one of

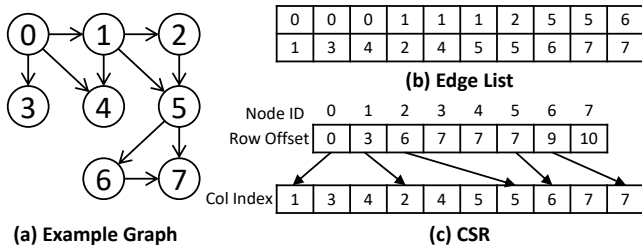


Figure 1: An example of CSR format.

the most frequently used graph format, which is to record each node’s out-degree neighbors compactly as illustrated in Figure 1. In CSR, E integers (assuming 32 bit integers) are needed to represent a graph. To further reduce the storage usage of the graph, we employ CGR so that each edge takes fewer than 32 bits.

In this work, graph data is stored in the CGR format, and it follows the three steps shown below to convert the raw graph data represented in the traditional adjacency list format into the CGR format: (i) Intervals and Residuals Representation, (ii) Gap Transformation, and (iii) VLC Encoding. In the following, we introduce some details about these three steps to facilitate our presentation on GPU graph traversal on CGR in subsequent technical sections.

Intervals and Residuals Representation. For many real-world graphs, the adjacency list of each node exhibits the locality characteristic to some extent. This means for a certain node, its neighbors do not distribute uniformly, but tend to form a number of clusters and the neighbors in the same cluster tend to have close indices. Hence, it is possible for the ordered neighbor sequence to form several sub-sequences with consecutive node indices, called intervals. As a consequence, we can denote a node’s adjacency list with two sequences, i.e., Intervals and Residuals Representation. For the neighbors covered in the sub-sequences with consecutive node indices in the adjacency list, we represent them as an interval with the starting node and the corresponding length. All intervals compose the interval sequence. For the neighbors which cannot form intervals, we need to record them separately in the residual sequence.

Gap Transformation. After Intervals and Residuals Representation, each node’s adjacency list is represented as an interval sequence and a residual sequence. For each sequence, we transform it into the differential sequence of the original sequence, that is to denote each element as the difference between itself and its preceding element. This process is called Gap Transformation. The target of Gap Transformation is to decrease the absolute value of each number in the sequence while maintaining the original information amount. After such transformation, we can record the equivalent sequence

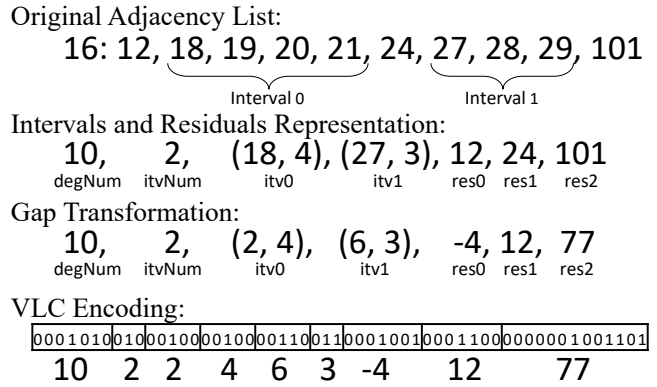


Figure 2: An example of CGR format.

information with fewer bits via the VLC encoding technique introduced below.

Variable-Length Code (VLC) Encoding. VLC is widely used in various data compression scenarios. Compared with fixed-length encoding, VLC can vary the number of bits needed to represent an element. VLC works well for compressing power-law graphs [8] since the distribution of elements in such graphs are skewed, in which case VLC uses a smaller number of bits to encode the more frequent elements in order to compress the overall size. We refer interested readers to Appendix B for some more details on VLC Encoding involved in this work.

To achieve better compression results, we combine the aforementioned approaches to encode the adjacency lists. An illustrative example is given as follows.

Example 3.1. In Figure 2, we demonstrate how to compress the adjacency list of node16 which has 10 neighbors. In its sorted form, the adjacency list contains 2 intervals and 3 individual nodes called residuals. We employ the encoding scheme as follows. First, this scheme stores the number of neighbors degNum in node16’s adjacency list. Then it records the number of intervals itvNum. Next, the encoding is followed by itvNum tuples and each tuple contains the starting node’s index and the interval length. In each interval, the starting node is represented using the gap value from the previous interval’s ending node, and the first interval’s starting node is denoted using the gap value from node16. Hence, the first interval’s starting node is node18 with a corresponding gap value (from node16) of 2. The second interval’s starting node is node27, and its gap value from the first interval’s ending node21 is 6. After these two intervals, this scheme encodes the remaining residuals (due to degNum, there is no need to record the number of residuals). Except for the first residual, which is represented with a gap value from node16, the other residuals are all described using gap values from the corresponding preceding residuals. Finally, this scheme

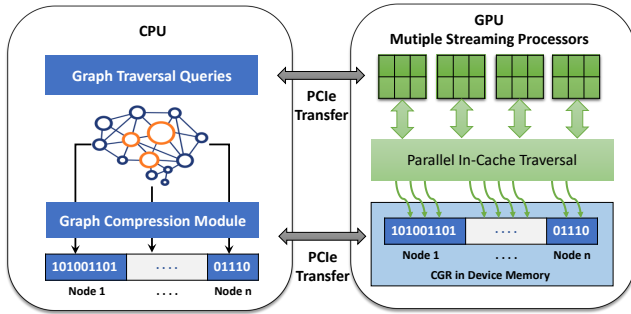


Figure 3: GCGT overview.

uses VLC to encode this node’s adjacency list from the compressed format explained above into a compressed bit array¹. From this example, we can find that the original adjacency list which requires 10 integers (i.e., 320 bits) in the representation, can be denoted with only 55 bits on CGR.

Furthermore, the compression rate is highly dependent on the *Node Reordering* techniques since they alter the locality property of the graph to be compressed. Given a graph $G = (V, E)$, node reordering is a bijection $\sigma : V \rightarrow V$, which assigns a new labelling to all nodes in the graph, i.e., $G' = (V, E' = \{(\sigma(v), \sigma(u)) | (v, u) \in E\})$. We employ several reordering algorithms in this work to improve the locality of graphs for higher compression rates, which will be discussed in Section 7 and Appendix D.

3.2 GCGT Overview

The overview of the proposed GCGT is illustrated in Figure 3. The graph is compressed in CPU and transferred to GPU’s device memory. CPU issues graph traversal queries (e.g., BFS) by invoking GPU kernels. GCGT allows the storing and processing of larger graphs on GPUs with the help of compression. Even when the compressed graph cannot entirely reside in the device memory, CGR reduces the PCIe transfer cost since we can directly move the compressed adjacency lists to GPUs and process them without decompression in the device memory. For graph processing, GCGT effectively hides the additional overhead of dealing with compressed data while traversing the graph, by leveraging massive parallel threads on GPUs. In each iteration of the traversal, a number of threads collaborate in processing the neighbor list of a frontier node and outputting qualified neighbors (e.g., unvisited nodes for BFS) to the frontier of the next iteration. It is noted that, for traversal on the CGR format, we only decode and process the adjacency lists in the cache of GPU’s cores. To achieve load balancing, we propose a number of novel strategies on dynamically assigning threads to collaborate, which will be extensively discussed in Sections 4 and 5.

¹We refer interested readers to Appendix C for the implementation details of CGR encoding.

4 GPU-BASED COMPRESSED GRAPH TRAVERSAL GCGT

Existing parallel graph traversal approaches on uncompressed graphs assume all neighbor nodes are immediately available for parallel processing. Hence, it is rather straightforward for existing approaches to predict the workload and launch appropriate number of threads that access the neighbor lists of frontier nodes concurrently. However, such assumption does not hold if the neighbor lists are encoded in VLC. VLC poses significant challenges for efficient graph traversal processing on GPUs since it is difficult to generate balanced workloads in the decoding stage (inherently serial) to feed massive threads on GPUs. Moreover, the architecture of GPUs does not favor complex scheduling to adjust the workloads dynamically.

Thus, in this section, we first introduce an intuitive solution which assigns threads to process compressed adjacency lists independently (Section 4.1). Subsequently, we propose a Two-Phase Traversal strategy which schedules the processing of the interval segments and residual segments into separate phases, so as to eliminate thread divergence caused by threads in the same warp entering different control logics of the interval and residual segments (Section 4.2). Finally, we devise a Task-Stealing optimization to deal with workload imbalance caused by processing in parallel adjacency lists with skewed lengths of residual segments (Section 4.3).

4.1 Parallel Graph Traversal on CGR

Typically, approaches for parallel graph traversal based on ping-pong frontier queues are executed in an iterative manner. The initial node(s) are placed into `INQUEUE` before the traversal starts. In each iteration, a thread takes its assigned frontiers from `INQUEUE`, inspects all neighbors from a frontier’s adjacency list, and then pushes any unvisited neighbors to `OUTQUEUE`. `OUTQUEUE` replaces `INQUEUE` for the new frontier queue in the next iteration. Intuitively, a natural solution for GCGT is to assign a thread to process the adjacency list of a frontier: each thread independently accesses the compressed bit arrays of the CGR-format adjacency lists (of those frontiers assigned to it), decodes the neighbors one by one and then pushes unvisited ones to `OUTQUEUE` if necessary.

We present this intuitive solution for GCGT in Algorithm 1. **Procedure BfsBasic** is the main procedure which aims to output the unvisited neighbors of `INQUEUE`’s frontiers to `OUTQUEUE`, and use them as the input frontiers in the next iteration. Since the algorithm runs in the SIMT manner, the same instructions are executed in parallel within a *thread group* and each thread’s behavior is characterized by `threadNum` (how many threads in the thread group) and `threadId` (the thread’s ID in the thread group). Each thread is assigned a frontier from `INQUEUE` according to its own `threadId` (i.e., `u` in line 4). The thread then decodes `u`’s compressed adjacency

Algorithm 1 Intuitive Solution for GCGT

```

1: procedure BFSBASIC(inQueue[], outQueue[])
2:   offset := 0
3:   while offset + threadIdx < inQueue.size do
4:     u := inQueue[offset + threadIdx]
5:     bitPtr := bitStart[u]
6:     degNum = decodeNum(bitPtr)
7:     while degNum-- do
8:       v := getNextNeighbor(u, bitPtr)
9:       appendIfUnvisited(v, outQueue)
10:    offset += threadIdx

11: function GETNEXTNEIGHBOR(u, bitPtr)
12:   if first call then
13:     itvNum := decodeNum(bitPtr)
14:     curItvPtr := u
15:     curItvLen := 0
16:     curRes := u
17:   if curItvLen then
18:     return curItvPtr++, curItvLen -- 1
19:   if itvNum then
20:     curItvPtr += decodeNum(bitPtr)
21:     curItvLen := decodeNum(bitPtr)
22:     itvNum -- 1, curItvLen -- 1
23:     return curItvPtr++
24:   return curRes += decodeNum(bitPtr)

25: procedure APPENDIFUNVISITED(v, outQueue[])
26:   __shared__ outputOffset
27:   flag := unvisited(v) ? 1 : 0
28:   scatter, total := exclusiveScan(flag)
29:   if threadIdx == 0 then
30:     outputOffset := outQueue.atomicAdd(total)
31:   if flag then
32:     outQueue[outputOffset + scatter] := v

```

list as if it is running in serial. When a neighbor (i.e., v in line 8) is decoded, the thread appends it to `OUTQUEUE` if the node is unvisited (line 9).

Function decodeNum maintains the position of the bit pointer (`bitPtr`), decodes a number from the compressed bit array as the returned value and then updates the position of `bitPtr`. **Function getNextNeighbor** demonstrates the process of decoding the adjacency list in a serial manner. Specifically, there are three possible scenarios when decoding the next neighbor: (i) in the middle of an interval (lines 17-18), (ii) in the beginning of an interval (lines 19-23), and (iii) in the residual segment (line 24).

The aforementioned functions handle the decoding process, where the threads operate on their own without any

conflicts. However, race condition occurs when multiple threads concurrently append nodes to update `OUTQUEUE` (line 9). **Function appendIfUnvisited** is a common technique to alleviate contention for concurrent frontier updates on GPUs [33]. The idea is to communicate between threads in the same CTA so as to reduce the number of atomic operations when outputting the unvisited nodes to `OUTQUEUE`. To be specific, each thread first marks its current node v as either visited (0) or unvisited (1) and then invokes **exclusiveScan**² to obtain the number of unvisited nodes to push to `OUTQUEUE` in the same CTA (i.e., total) as well the outputting position in `OUTQUEUE` for each thread (i.e., scatter). The contention is reduced since only one thread from the CTA calls an atomic operation to allocate the space in `OUTQUEUE` while other threads can safely push their updates without locking.

4.2 Two-Phase Traversal

We would like to highlight that the intuitive solution presented in Algorithm 1 is rather expensive to deploy on GPUs due to severe thread divergence caused by **Function getNextNeighbor**. Since all adjacency lists are divided into interval and residual segments, it is likely that two threads in the same warp working on different types of segments try to get their next neighbor decoded simultaneously. As a consequence, these two threads should end up in diverging branches of **Function getNextNeighbor**. Given that any warp executes instructions in a physically synchronous manner on GPUs, the threads decoding the interval segments are completely idle waiting for threads decoding the residual segments to finish. In order to alleviate thread divergence, we propose a Two-Phase Traversal strategy to decode the adjacency lists, where we handle the interval segment and the residual segment in two separate phases.

We present the Two-Phase Traversal strategy in Algorithm 2. The decoding of the interval segment and that of the residual segment are handled by **Procedure handleIntervals** and **Procedure handleResiduals** respectively. **Procedure handleIntervals** calls **Procedure expandInterval** to expand each interval collaboratively by a thread group (line 16). Algorithm 2 has two distinguishing advantages over Algorithm 1: (1) better memory access patterns: a thread group jointly handles consecutive neighbors of one interval at a time, whereas each thread in Algorithm 1 independently loads different intervals causing uncoalesced memory accesses; (2) less thread divergence: **Procedure expandInterval** synchronizes the thread group once an interval is

²**Function exclusiveScan** is a common primitive on GPUs. When called by multiple threads, it will see the arguments from each thread as an array ordered according to `threadId`, and then compute the prefix sum of the array. There are two returned values, `scatter` and `total`, representing `sum(input[0..threadId-1])` and `sum(input)` respectively.

Algorithm 2 GCGT Two-Phase Traversal

```

1: procedure TWOPHRASE(inQueue[], outQueue[])
2:   offset := 0
3:   while offset + threadId < inQueue.size do
4:     u := inQueue[offset + threadId]
5:     bitPtr := bitStart[u]
6:     degNum = decodeNum(bitPtr)
7:     handleIntervals(u, degNum, bitPtr)
8:     handleResiduals(u, degNum, bitPtr)

9: procedure HANDLEINTERVALS(u, degNum, bitPtr)
10:  itvNum := decodeNum(bitPtr)
11:  curItvPtr := u
12:  while itvNum-- do
13:    curItvPtr += decodeNum(bitPtr)
14:    curItvLen := decodeNum(bitPtr)
15:    degNum -= curItvLen
16:    expandInterval(curItvPtr, curItvLen)

17: procedure HANDLERESIDUALS(u, degNum, bitPtr)
18:  curRes := u
19:  while degNum-- do
20:    curRes += decodeNum(bitPtr)
21:    appendIfUnvisited(curRes, outQueue)

22: procedure EXPANDINTERVAL(curItvPtr, curItvLen)
23:  __shared__ winnerId
24:  while syncAny(curItvLen ≥ threadNum) do
25:    if curItvLen ≥ threadNum then
26:      winnerId := threadId
27:      winnerItvPtr := shfl(curItvPtr, winnerId)
28:    if winnerId == threadId then
29:      curItvPtr += threadNum
30:      curItvLen -= threadNum
31:      v := winnerItvPtr + threadId
32:      appendIfUnvisited(v, outQueue)
33:  __shared__ neighbors[threadNum]
34:  scatter, total := exclusiveScan(curItvLen)
35:  progress := 0
36:  while progress < total do
37:    while scatter < progress + threadNum do
38:      if curItvLen == 0 break
39:      neighbors[scatter - progress] = curItvPtr
40:      scatter++, curItvPtr++, curItvLen--
41:      v := neighbors[threadId]
42:      appendIfUnvisited(v, outQueue)
43:      progress += threadNum

```

decoded, which protects any threads from entering **Procedure handleResiduals** ahead of other threads in the same group and causing diverging behavior thereafter.

We further divide **Procedure expandInterval** into two stages. In the first stage, a thread group focuses on processing a long interval (lines 23-32). In the second stage, these threads collaboratively process multiple short intervals (lines 33-43).

In the first stage, if the length of an interval being discovered by a certain thread exceeds threadNum, we can then leverage the entire thread group to handle the interval as there is sufficient workload assigned. Thus, this particular thread needs to lead its thread group to expand the interval. The leader election is achieved through **Function syncAny** and **Function shfl**, two thread synchronization primitives³ on GPUs. To be specific, **Function syncAny** returns true if any thread discovers an interval longer than threadNum, and all threads will enter the first while loop to vote for a leader. Subsequently, each leader candidate participates in the resource competition through writing its own threadId to the shared variable winnerId (lines 25-26). The leader information as well as the starting node of the assigned interval is then broadcast to the thread group through **Function shfl** (line 27). When the broadcast ends, all threads can now collaborate in decoding the interval discovered by the leader thread. Based on the starting node of the interval, each thread retrieves the assigned node and outputs unvisited neighbors to OUTQUEUE (lines 31-32).

In the second stage, the remaining length of intervals held by all threads cannot occupy their corresponding thread group. To make more threads participate, we need to handle multiple intervals in a collaborative manner. The thread group synchronizes the interval information for collaboration through **Function exclusiveScan**, where each thread notifies others on the remaining length of its interval (line 34). Next, the thread group processes threadNum neighbors in each round of the second while loop (lines 36-43). Within the nested loop, the qualified threads exclusively write their next neighbor based on the offset calculated by the **Function exclusiveScan** to fill the shared memory buffer with threadNum neighbors (lines 37-40). This nested loop thus generates enough workloads for the thread group to output the decoded neighbors to OUTQUEUE (lines 41-42).

In the sequel, we present an example to simulate the execution of the Two-Phase Traversal strategy, so as to further clarify its advantages over the intuitive solution described in Algorithm 1.

Example 4.1. In Figure 4(a), we present a scenario where a warp consists of 8 threads and each thread is assigned to a frontier. The compressed format of a frontier's adjacency list follows the representation described in Section 3.1. In

³<https://devblogs.nvidia.com/using-cuda-warp-level-primitives/>

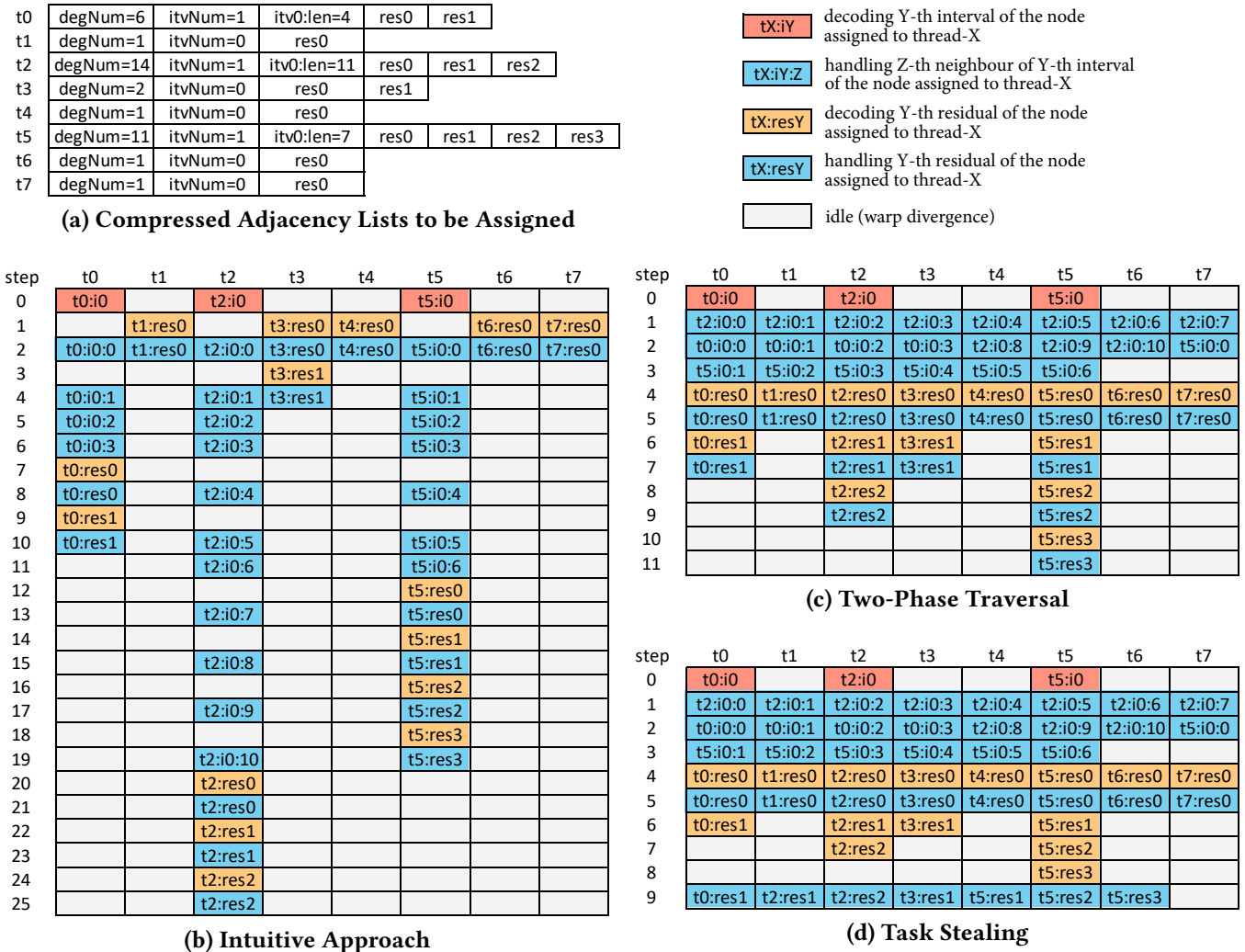


Figure 4: Instruction flow sequences of three approaches based on an example.

this particular scenario, the frontiers held by threads t0, t2 and t5 contain an interval whereas the rest of the frontiers only contain residuals. Figure 4(b) illustrates the instruction flow sequences of Algorithm 1. To simplify the presentation, an instruction could be decoding an interval, decoding a residual or checking whether a node is visited. This simplification makes sense because these operations require device memory accesses, which are the major cost considered in the context of GPU-based graph processing. Furthermore, we choose different colors to highlight the types of instructions executed by a thread at a time. Note that the threads must execute the same instruction in the SIMT manner thus the colors will be the same for each step; otherwise, the threads are idle. As shown in Figure 4(b), if the threads do not collaborate with each other but only divide tasks based on frontiers, each thread will decode and process one neighbor at a time.

As a consequence, severe thread divergence occurs for two major reasons: (a) a few threads decode long adjacency lists resulting in load imbalance (t2 and t5) and unnecessarily occupy a significant amount of GPU resources, e.g., registers; (b) threads are running diverging instructions for different types of operations.

In contrast, we illustrate the instruction flow sequence for the Two-Phase Traversal strategy in Figure 4(c). In step 0, t0, t2 and t5 read their respective intervals' information. As the length of interval held by t2 is larger than threadNum (i.e., $itvLen = 11 > (threadNum = 8)$), t2 leads all threads to process the first threadNum neighbors of the interval (Algorithm 2, lines 23-32). After that, the length of the interval held by t2 is decreased to 3, and there is no thread holding an interval long enough to occupy all threads. Therefore, the algorithm finishes processing long intervals and enters

Algorithm 3 GCGT Task Stealing

```

1: procedure HANDLERESIDUALS+(u, degNum, bitPtr)
2:   curRes := u
3:   while syncAll(degNum) do
4:     curRes += decodeNum(bitPtr)
5:     appendIfUnvisited(curRes, outQueue)
6:     degNum--
7:   __shared__ neighbors[threadNum]
8:   scatter, total := exclusiveScan(degNum)
9:   process := 0
10:  while progress < total do
11:    while scatter < progress + threadNum do
12:      if degNum == 0 break
13:      curRes += decodeNum(bitPtr)
14:      neighbors[scatter - progress] := curRes
15:      scatter++, degNum--
16:      v := neighbors[threadId]
17:      appendIfUnvisited(v, outQueue)
18:      progress += threadNum

```

the stage to process short intervals. Subsequently, t_0 , t_2 , t_5 obtain the scatter values 0, 4, 7 respectively so that they can later push their interval workloads to the shared memory for all threads to collaborate. In each round, the corresponding threads put the neighbors in the shared array, and then all threads retrieve the assigned neighbor for processing. It is noted that the interval segments are handled in steps 2-3 and the residual segment are handled in steps 4-11. Apparently, the Two-Phase Traversal strategy reduces the thread divergence issue, particularly for scheduling the threads to process the interval segments collaboratively, which results in fewer execution steps compared with those of Algorithm 1.

4.3 Task Stealing

One can observe from Figure 4(c) that, even though the workloads of processing interval segments are balanced among threads, the decoding of residual segments still leads to imbalanced workloads. Unlike interval segments where the nodes in the interval can be immediately calculated according to the starting node and the length of the interval, the residual segments have to be decoded one by one serially since the encoding of a node is strictly dependent on its preceding nodes. When the distribution w.r.t. the length of the residual segment held by each thread is skewed, a large number of threads are idle waiting for the large residual segment to finish. We thus devise the Task-Stealing strategy to make the idle threads work on the unfinished residual segments. The strategy is depicted in **Procedure handleResiduals+** of Algorithm 3. We schedule the processing of residual segments in two stages. In the first stage, all threads process their own

Algorithm 4 Parallel VLC Decoding

```

1: function PARALLELDECODE(bitPtr, results[])
2:   __shared__ vals[threadNum]
3:   __shared__ poss[threadNum]
4:   __shared__ flags[threadNum]
5:   myBitPtr = bitPtr + threadId
6:   vals[threadId] := decodeNum(myBitPtr)
7:   poss[threadId] := myBitPtr - bitPtr
8:   flags[threadId] := threadId ? 0 : 1
9:   while true do
10:    flag := flags[threadId]
11:    pos := poss[threadId]
12:    if syncNone(flag && pos < threadNum) break
13:    if pos < threadNum then
14:      if flag then flag[pos] := 1
15:      poss[threadId] := poss[pos]
16:    scatter, total := exclusiveSum(flag)
17:    if flag then results[scatter] := val
18:    return total

```

workloads until one finishes. In the second stage, the remaining threads write their decoded neighbors to the shared memory so that other threads can steal the workloads and collaboratively push the updates to `OUTQUEUE`. Figure 4(d) continues Example 4.1 by demonstrating the effectiveness of the Task-Stealing strategy. In this example, the idle threads before processing the residual segments are t_1 , t_4 , t_6 and t_7 . They effectively steal the workloads from other threads and collaboratively write decoded neighbors to `OUTQUEUE` in step 9. Compared with Figure 4(c), the Task-Stealing strategy further saves two execution steps.

5 OPTIMIZATIONS FOR POWER-LAW GRAPHS

We note that most real-world graphs follow the power-law distribution. Under these circumstances, the residual sequences of the high-degree nodes are significantly longer than those of the rest of the nodes. As a consequence, only a small number of thread groups are scheduled to work on long residual sequences and the GPU resources are vastly wasted.

In Section 5.1, we propose a novel warp-centric decoding approach to concurrently decode one encoded residual bit array by falling back on idle threads, with a theoretical guarantee on the number of scans. In Section 5.2, we introduce the residual segmentation traversal to deal with long sequences of residuals in power-law graphs. We partition a long sequence of residuals into multiple segments, which breaks the sequential dependencies between the residuals for parallel processing.

5.1 Warp-centric Decoding

One straightforward scheduling for processing multiple encoded residual sequences in parallel is to assign a thread to each node. However, skewed graphs lead to frequent thread starvation. In the meanwhile, threads in a warp decoding their nodes' residuals independently incur uncoalesced memory accesses (reading bit arrays in different memory locations) and warp divergence (entering different control branches for VLC decoding). Hence, we introduce a warp-centric approach. It is challenging to enable parallel decoding as it is not possible to obtain the position of a residual before decoding its predecessors in the residual sequence.

To solve this challenge, we consider concurrently decoding multiple VLCs which are encoded in a bit array with a group of threads. Since the beginning bit position of each VLC encoding is unknown in advance, we assign a thread to start from each bit position. Each thread then decodes a number according to its beginning bit position. Apparently, only the decodings of those threads starting from a real VLC beginning position are valid, so it is required to identify which decodings are valid among all decoded candidates.

To achieve the best warp efficiency for decoding VLC bit arrays in parallel, we present the following approach in Algorithm 4. First, a warp of threads tries to conduct decoding on every position in a consecutive area as the beginning bit (lines 5-6). Next, for each thread, we can get the decoded number if we decode from the corresponding bit position, and the bit position after decoding (i.e., the beginning bit position of the next encoding, lines 6-7). It is important to know which threads hold valid decodings. Given that thread-0 which starts from the first bit position gets a valid decoding for sure, and the lengths of decoded bits of each thread are available, we can concatenate all valid decodings starting from thread-0.

Instead of serially marking valid decodings one at a time, based on the SIMT execution, we can mark candidates at an exponential rate, meaning that every marked thread can mark a new valid decoding at each round. Hence, we can design an efficient approach of selecting valid decodings with a complexity of $O(\log_2 \text{threadNum})$ (lines 9-16), which could possibly yield threadNum decoded nodes in parallel. We illustrate this process in an example as follows.

Example 5.1. As shown in Figure 5, suppose a thread group contains 16 threads and the thread group is used to decode the bit array (as illustrated in the figure) which is in γ -code⁴, and the encoded numbers in the bit array are from 1 to 5 in order. First, 16 threads start to decode from 16 bit positions, and then obtain the number (decoded starting from the corresponding bit position) and the beginning bit position of

⁴We refer interested readers to Appendix B for details about VLC encoding including γ -code.

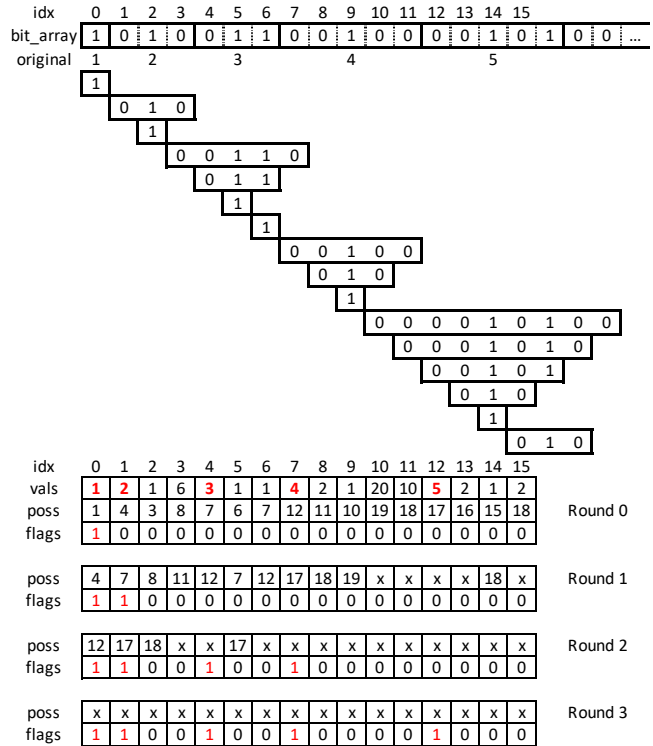


Figure 5: An example of parallel VLC decoding.

the next encoding, i.e., vals and poss in Round 0 as illustrated in Figure 5. After that, we aim to identify all valid decodings, i.e., 1, 2, 3, 4, 5 (highlighted in red) which are held by thread-0, 1, 4, 7, 12.

In Round 0, only flags[0] is 1 while the others are 0, meaning that, initially, we can only be sure that the number decoded by thread-0 is valid. In the next several rounds, each marked thread will mark a new thread which holds valid encodings according to pos in each round, and then update their own pos to the next index of thread to be marked. For instance, in Round 0, flags[0] is 1 and poss[0] points to thread-1 so that thread-1 is marked by thread-0. Then, the pos is assigned to "the pos of pos" which updates indices of threads to be marked in the next round. Next, in Round 1, thread-0, 1 will respectively mark thread-4, 7 according to the updated pos. Consequently, in Round n, pos points to the beginning bit position of the subsequent 2ⁿ-th valid encoding. The threads which have been marked with a valid encoding, will mark a new valid encoding according to this pos, unless the pos exceeds the threadNum.

LEMMA 5.2. Given a warp composed of K threads to decode VLCs starting from K consecutive bits in parallel, the computational complexity to identify all valid VLC decodings among K candidates is $O(\log_2 K)$.

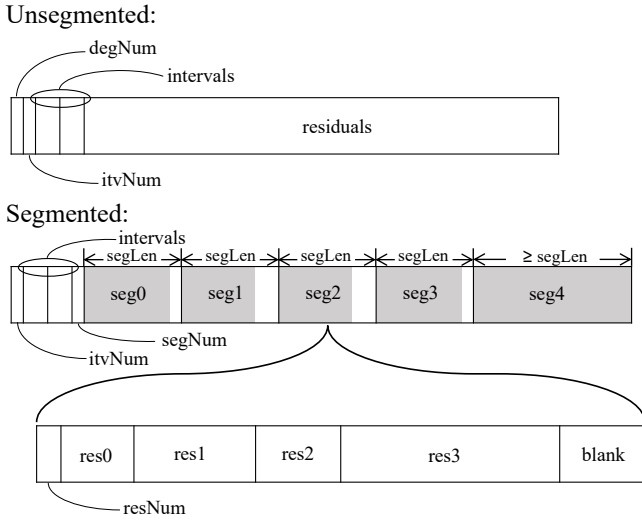


Figure 6: Compressed data format after segmenting compressed residuals.

PROOF. Let pos_i denote the position of the next valid decoding to be marked by thread- i , if thread- i is marked. Initially, in Round 0, pos_i points to the position where thread- i just finishes its decoding, i.e., the first valid starting position after thread- i 's decoding. Naturally, thread-0 is marked.

Before Round n starts, the first 2^n valid decodings are marked. Assume thread- i is the j -th marked thread, then pos_i points to the $(2^n + j)$ -th valid decoding. Hence, in this round, the valid decodings from the 2^n -th to the 2^{n+1} -th will be marked. After that, pos_{pos_i} is assigned to pos_i , so that pos_i points to the $(2^{n+1} + j)$ -th valid decoding.

Finally, after Round n , the first 2^{n+1} valid decodings will be identified. There are at most K candidates, so we conclude that the complexity is $O(\log_2 K)$. \square

Given the property that threads in a warp are naturally synchronized and the corresponding communication cost is very low, the main bottleneck of the collaboration within the warp lies in memory accesses. When there are enough active warps which can fully occupy the memory bandwidth, we can trade some instruction executions for higher parallelism.

5.2 Residual Segmentation

The proposed GCGT processes graph traversal in a node-centric parallel manner. However, we note that there exist some nodes whose residual sequences are remarkably longer than those of other nodes in real-world graphs. This leads to low parallelism and degraded performance. To achieve a better load balancing, we divide a long residual sequence into smaller segments for a fine-grained workload partitioning.

In Figure 6, we illustrate the compressed data format after segmenting compressed residuals. We divide a node's data into two parts: the first part corresponds to the interval area,

starting with $itvNum$, followed by the starting nodes and lengths of $itvNum$ intervals. Then the second part is the residual area, starting with $segNum$ denoting how many following segments there are. We assume a parameter $segLen$ as the basis of segmenting the residual area. If the residual area is long enough, the length of all segments is strictly $segLen$, except for the last segment. We try to place as many residuals as possible in each segment, and if we cannot fully fill the segment up, we will leave the remaining space as blank. The advantage of this strategy lies in that, when reading $segNum$, we immediately know the corresponding bitPtr of the following $segNum$ residuals according to $segNum$ and $segLen$. Therefore, we can proceed with the multi-way processing with at most $segNum$ threads. The $segLen$ involved is an important parameter. Obviously, a smaller $segLen$ leads to a larger $segNum$, so that more threads can participate in processing this super-long residual area in parallel. However, this will at the same time, cause the sum of each segment's blank area to be larger, waste more space, and decrease the compression rate. Therefore, $segLen$ is a trade-off between the compression rate and the computational efficiency. We will explore this trade-off in Appendix D.

For each residual segment, we first record $degNum$ representing the number of residuals in the segment. This is followed by the residuals in order with the corresponding gap values. When we cannot place more residuals, we leave the remaining space as blank and these $segLen$ bits compose a segment. Note that it is unnecessary for the last segment to have blank area or to be aligned. Specifically, in order to reduce the space waste as much as possible, we require that during segmentation, the length of the last segment should be larger than $segLen$ (its bit length should be 1-2 times of $segLen$, instead of dividing the last part to be a segment shorter than $segLen$).

6 GCGT EXTENSIONS TO OTHER GRAPH APPLICATIONS

The proposed techniques of GCGT can be extended to other graph applications. GCGT falls into the category of node-centric parallel graph processing, which iteratively executes a pipeline of *expansion - filtering - contraction* on the ping-pong frontier queue (as illustrated in Figure 7(a)). Take BFS for an example, we first perform expansion for all neighbor nodes connected to one of the frontier nodes, and then check each neighbor if it is visited (specific for BFS) in the filtering step. If a neighbor is unvisited, we update the label of the node and keep it for the next iteration (as shown in Figure 7(b)). There exists a large number of graph applications that can fit into the expansion - filtering - contraction computational pipeline [47]. GCGT can be easily extended to these applications by adapting the filtering step. We take two

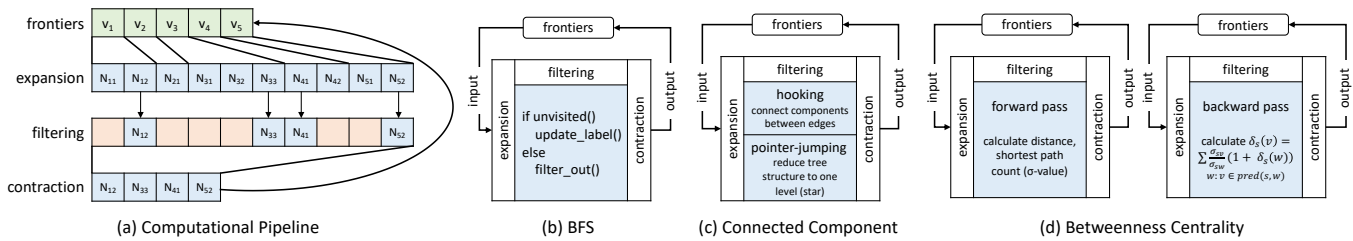


Figure 7: Computational pipeline and implementation details of multiple applications.

important graph applications, i.e., CC (Connected Component) and BC (Betweenness Centrality), to demonstrate the generality of GCGT.

Connected Component assigns a component ID for each node, such that the nodes assigned to the same component ID are connected in the graph. J. Soman et al. [42] propose the state-of-the-art approach of CC on GPUs, which includes two kernels, i.e., hooking and pointer-jumping, to achieve the disjoint-set forests [19] in a parallel manner. These two kernels can be employed in GCGT pipeline as shown in Figure 7(c). In the filtering step, we first check if each expanded neighbor belongs to the same component ID (in the same component tree) as the corresponding frontier. If not, the component tree root of one node is linked to that of the other’s (hooking). Subsequently, we re-direct all nodes on the tree path to the root to flatten the component tree to one level only (pointer-jumping). If a node and all its neighbors belong to the same connected component, it will be excluded in the filtering step and will not enter the next iteration.

Betweenness Centrality measures the centrality of a particular node based on the percentage of its occurrences in shortest paths among all node pairs. A. Sriram et al. [44] propose a widely-used approach to calculate BC on GPUs, which needs two passes for traversing the graph. In the forward traversal pass, the distance label and the shortest path count (defined as σ -value) between each node in the graph and the source node are calculated. In the backward traversal pass, we traverse all nodes based on the distance label (obtained in the forward pass) in the descending order, to calculate δ -value and then derive BC value based on the Brandes’s formulation [9]. σ and δ can be easily computed in the filtering step of two separate kernels as shown in Figure 7(d).

In this paper, we also evaluate the performance of GCGT extensions to CC and BC in Appendix E.

7 EXPERIMENTAL EVALUATION

In this section, we present the experimental evaluation of the proposed GCGT scheme. Section 7.1 describes the experimental setup. Section 7.2 presents our main results: comparing GCGT with the state-of-the-art CPU-based and GPU-based parallel graph traversal approaches in order to evaluate GCGT’s effectiveness on accelerating graph analysis on CGR. Section 7.3 verifies the impact of each proposed technique

on the performance in each dataset. We also evaluate the sensitivity of the parameters used in GCGT and demonstrate the efficiency of GCGT extensions to CC and BC. We refer interested readers to Appendix D and E respectively.

7.1 Experimental Setup

Datasets. We collect two web graph datasets (uk-2002 and uk-2007), two social network graph datasets (ljournal and twitter) and one biology graph dataset (brain). The details of these datasets are described as follows and the statistics are summarized in Table 1.

- uk-2002 is a web graph dataset obtained in 2002. It is crawled from the web pages which belong to .uk domain by UbiCrawler [4].
- uk-2007 is a web graph dataset extracted by DELIS [6]. It is a monthly snapshot (2017-5) which is also specific to .uk domain.
- ljournal is a social network graph representing the friendship relationship of LiveJournal⁵, which is a free online blog service involving millions of users. This dataset is a snapshot collected in 2008 [12].
- twitter contains the relationship between users and followers in Twitter⁶. It is a snapshot collected in 2010 via Twitter API by [27].
- brain is an undirected network representing the link structure among neurons of human beings’ brain. It is collected by NeuroData⁷ and provided by NetworkRepository⁸.

Graph Traversal Approaches. To evaluate our proposal, we compare it with several state-of-the-art CPU-based and GPU-based graph traversal approaches.

- Naïve (CPU). The single-threaded implementation, which provides a basic reference for the traversal performance.
- Ligra [40] (CPU). The state-of-the-art parallel graph processing framework for a single multi-core machine.
- Ligra+ [41] (CPU). The subsequent variant of Ligra, which supports graph processing on compressed graphs.
- Gunrock [47] (GPU). The state-of-the-art graph analytic platform designed specifically for GPUs.

⁵<https://www.livejournal.com/>

⁶<https://twitter.com/>

⁷<https://neurodata.io/data/>

⁸<http://networkrepository.com/bn-human-Jung2015-M87113878.php>

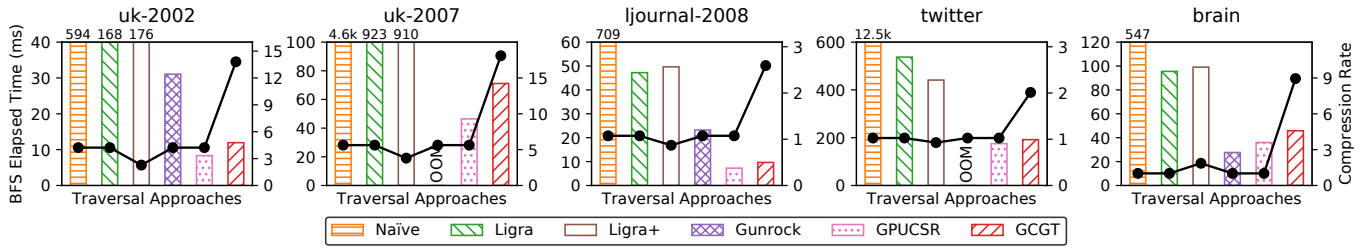


Figure 8: BFS Elapsed Time and Compression Rate comparison between GCGT and multiple baselines.

Table 1: Statistics of Datasets

Datasets	Category	$ V $	$ E $	$ E / V $
uk-2002	Web	18.5M	298M	16.1
uk-2007	Web	105M	3.73B	35.5
ljournal	Social Network	5.3M	79M	14.9
twitter	Social Network	41.6M	1.46B	35.1
brain	Biology	784K	267M	683

Table 2: Selected Parameters

Parameter	Value
VLC sheme	ζ_3 -code
Min Interval Length	4
Node Reordering	LLP [5]
Residual Segment Length	32 bytes

- GPUCSR (GPU). The state-of-the-art GPU-based standalone implementation on the traditional CSR format for each particular application. To be specific, it refers to D. Merrill et al. [33] (BFS), J. Soman et al. [42] (CC), and A. Sriram et al. [44] (BC) respectively⁹.
- GCGT (GPU). The proposed approach for GPU-based graph traversal on compressed graphs.

Experimental Environment. All experiments are conducted on a two-way Xeon server, with two Intel Xeon Gold 6140 Processors (36 cores, 2.3Hz) and 256GB main memory. The machine has a NVIDIA TITAN V GPU (5120 Cores and 12GB device memory). All source codes are compiled by GCC-7.3 and CUDA 10.0 in C++14 standard with -O3. OpenMP is used to provide parallel primitives for Ligra and Ligra+.

7.2 Comparison Results Analysis

We demonstrate the main results by comparing GCGT with all baselines introduced in Section 7.1. We configure GCGT with the parameter setting described in Table 2, as we find it leads to the best overall performance across datasets. We discuss the parameter sensitivity in Appendix D.

Evaluation Criterion. We consider two metrics when evaluating GCGT: (i) memory usage saved when storing graph data into the CGR format, (ii) computational overhead caused by GCGT decoding on the CGR format. A unified preprocessing is conducted in each dataset before running any experiment, i.e., restructure the original graph by virtual node compression [10] and then reorder nodes' indices [5] to improve the locality. For each evaluated approach, we execute BFS 100 times starting from a randomly selected node and calculate the average result to evaluate the elapsed time of the computation. The results are shown in Figure 8. We use *bar* plots to denote each approach's elapsed time of graph traversal.

⁹Please note that the experimental results of CC and BC are discussed in Appendix E.

The corresponding label is on the left of y-axis with the unit of millisecond (ms). Meanwhile, the compression rates (i.e., 32 / bits per edge) are illustrated in *line* plots with black dots. A larger compression rate leads to smaller memory usage. The corresponding label is on the right of y-axis. It is noted that the purpose of introducing the two metrics into one plot is to demonstrate the trade-off between efficiency and memory usage for each compared approach, which is the main concern of this paper:

- How much device memory will be saved if storing graphs on CGR which GCGT can operate directly on?
- Compared with approaches traversing on uncompressed graphs, how efficient is GCGT?

Compression Rate Evaluation. For a particular dataset, Naïve, Ligra, Gunrock, and GPUCSR share the same compression rate, since they all benefit only from virtual node compression in the dataset preprocessing. It is worth noting that, Ligra+ further compresses the graph into byte-RLE, and GCGT further compresses the graph into CGR. The virtual node compression only works well on web graphs. In graphs after virtual node compression, Ligra+ (byte-RLE) can only further improve the compression rate on brain, mainly because its $|V|$ is smaller than others.

In contrast, CGR demonstrates high compression rates across datasets. For the web graphs and brain, more than 10x compression rates are achieved, which translates to only 1-2 bits per edge. For the social network datasets, GCGT also achieves a compression rate of 2x-3x.

We would like to highlight that the compression rate varies across datasets from different domains. A network can be effectively compressed if it renders good locality characteristic: neighbors of any node have IDs close to each other. When considering brain, which shows a hierarchical structure with distinguishable clusters, it infers better locality and hence this type of networks is compression-friendly to

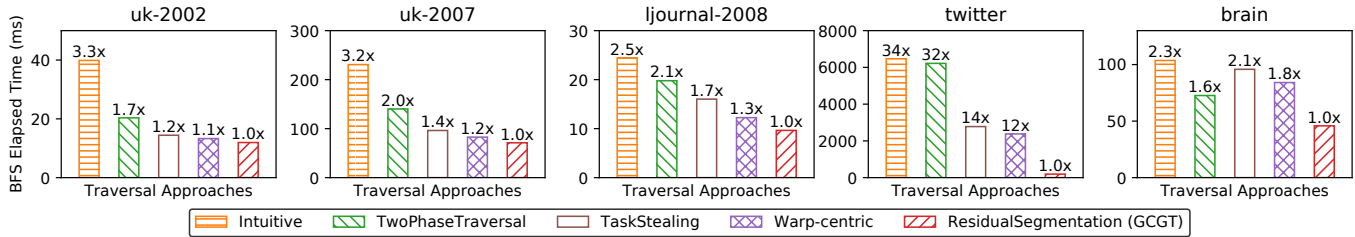


Figure 9: Optimization impact analysis results.

the CGR format. For the web graph, on one hand, the neighbors share high similarity (e.g., pages belonging to the same website); on the other hand, the data of the web graph are collected with crawlers following hyper-links. Thus the collected data corresponds to a subset of websites with high locality. In contrast, the data collection of social networks generally follow the time-line, and the sampling frequency is constrained by service providers (e.g., Twitter Streaming API only provides no more than 1% tweets for collection). Hence, the locality characteristic in the graph structure is destroyed to a certain extent in the process of data collection. Hence, poor locality degrades the effectiveness of CGR.

Traversal Elapsed Time Evaluation. When comparing CPU-based and GPU-based approaches, we verify that the GPU is an appealing accelerator for graph analysis, i.e., GPU-based approaches (Gunrock, GPUCSR and GCGT) are significantly faster than CPU-based approaches (Ligra and Ligra+).

The comparison between GPUCSR and GCGT is interesting in the sense that it demonstrates the trade-off between performance and device memory usage. Compared with GPUCSR based on traditional non-compressed graph format, we can see that GCGT incurs a very low overhead of decoding while traversing the graph. In the worst case of uk-2007, 18.1x compression rate is achieved at the expense of introducing 54% latency overhead. Finally, Gunrock faces the out of memory (OOM) issue on larger datasets (uk-2007 and twitter), because it runs out of the 12GB device memory due to extra device memory allocated for its platform design.

Summary. These results have validated the motivation of conducting graph analysis directly on CGR, which significantly reduces the device memory pressure for GPU-based graph processing. Considering the high compression rates achieved, the performance reduction in terms of latency introduced by GCGT is promising, which is only a few ms in absolute time. In a nutshell, the compression would not only enable the analysis on much larger graphs, but also maintains the superiority of GPU-accelerated graph analysis over CPU counterparts.

7.3 Optimization Impact Analysis

In order to verify the effectiveness of each proposed optimization technique on the performance, we apply the techniques incrementally and illustrate the experimental results in Figure 9. We have the following interesting observations

through analyzing different datasets. *TwoPhaseTraversal* aims to avoid warp divergence when threads fall into different logic branches: executing either interval or residual decoding. As a result, the impact of *TwoPhaseTraversal* is effective in the web graphs with good locality (with many neighbors represented by intervals). *TaskStealing* is useful in the situation when the residual numbers vary significantly. *Warp-Centric* shows a relatively stable improvement for its better hardware utilization, and poses a larger impact when the average bits per edge are fewer, e.g., compared with 9% improvement achieved in uk-2002 (2.31 bits/edge), *Warp-centric* accelerates 16% in uk-2007 (1.17 bits/edge), and this is the same case in social network graphs. Note that brain is different from other datasets since its out-degree distribution is relatively uniform and its average out-degree per node is large. Hence, the overhead in thread collaboration in *TaskStealing* is not covered by the cycles saved, which results in the performance degradation after adding *TaskStealing*. As mentioned above, twitter exhibits a severe skewed distribution and thus, the execution is bottlenecked by several nodes with an extremely large out-degree. As a consequence, the effectiveness of *ResidualSegmentation* is significant in twitter.

8 CONCLUSION

In this paper, we introduce compressed graphs into GPU-based graph computation for optimized device memory usage, and propose GPU-based graph traversal on compressed graphs. First, we propose GPU-oriented parallel scheduling strategies, *Two-Phase Traversal* and *Task Stealing*, to fully utilize GPU’s computing resources without explicit decompression into global memory of GPUs. Second, to alleviate the issue of load imbalance in power-law graphs, we devise novel techniques including *Warp-centric Decoding* and *Residual Segmentation*. Finally, we evaluate the effectiveness and compatibility of the proposed GCGT through extensive experiments in representative graphs.

9 ACKNOWLEDGEMENT

We thank the anonymous reviewers for their insightful comments to improve the paper. The project is partially supported by a MoE Tier 2 grant (MOE2017-T2-1-141) in Singapore. Yuchen’s work is in part supported by a MoE Tier 1 grant (MSS18C001) in Singapore.

REFERENCES

- [1] Alberto Apostolico and Guido Drovandi. 2009. Graph Compression by BFS. *Algorithms* 2, 3 (2009), 1031–1044.
- [2] Jiri Barnat, Petr Bauch, Lubos Brim, and Milan Ceska Jr. 2011. Computing Strongly Connected Components in Parallel on CUDA. In *IPDPS*. 544–555.
- [3] Tal Ben-Nun, Michael Sutton, Sreepathi Pai, and Keshav Pingali. 2017. Groute: An Asynchronous Multi-GPU Programming Model for Irregular Computations. In *PPoPP*. 235–248.
- [4] Paolo Boldi, Bruno Codenotti, Massimo Santini, and Sebastiano Vigna. 2004. UbiCrawler: a scalable fully distributed Web crawler. *Softw., Pract. Exper.* 34, 8 (2004), 711–726.
- [5] Paolo Boldi, Marco Rosa, Massimo Santini, and Sebastiano Vigna. 2011. Layered label propagation: a multiresolution coordinate-free ordering for compressing social networks. In *WWW*. 587–596.
- [6] Paolo Boldi, Massimo Santini, and Sebastiano Vigna. 2008. A large time-aware web graph. *SIGIR Forum* 42, 2, 33–38.
- [7] Paolo Boldi and Sebastiano Vigna. 2004. The webgraph framework I: compression techniques. In *WWW*. 595–602.
- [8] Paolo Boldi and Sebastiano Vigna. 2004. The WebGraph Framework II: Codes For The World-Wide Web. In *DCC*. 528.
- [9] Ulrik Brandes. 2001. A faster algorithm for betweenness centrality. *J. Math. Sociol.* 25, 2 (2001), 163–177.
- [10] Gregory Buehrer and Kumar Chellapilla. 2008. A scalable pattern mining approach to web graph compression with communities. In *WSDM*. 95–106.
- [11] Gregory Buehrer, Roberto L. de Oliveira Jr., David Fuhry, and Srinivasan Parthasarathy. 2015. Towards a parameter-free and parallel itemset mining algorithm in linearithmic time. In *ICDE*. 1071–1082.
- [12] Flavio Chierichetti, Ravi Kumar, Silvio Lattanzi, Michael Mitzenmacher, Alessandro Panconesi, and Prabhakar Raghavan. 2009. On compressing social networks. In *KDD*. 219–228.
- [13] Francisco Claude and Gonzalo Navarro. 2010. Fast and Compact Web Graph Representations. *ACM Trans. Web* 4, 4 (2010), 16:1–16:31.
- [14] Laxman Dhulipala, Igor Kabiljo, Brian Karrer, Giuseppe Ottaviano, Sergey Pupyrev, and Alon Shalita. 2016. Compressing Graphs and Indexes with Recursive Graph Bisection. In *KDD*. 1535–1544.
- [15] Nhat Tan Duong, Quang Anh Pham Nguyen, Anh Tu Nguyen, and Huu-Duc Nguyen. 2012. Parallel PageRank computation using GPUs. In *SolCT*. 223–230.
- [16] Peter Elias. 1975. Universal codeword sets and representations of the integers. *IEEE Trans. Inf. Theory* 21, 2 (1975), 194–203.
- [17] Zhisong Fu, Harish Kumar Dasari, Bradley R. Bebee, Martin Berzins, and Bryan B. Thompson. 2014. Parallel Breadth First Search on GPU clusters. In *BigData*. 110–118.
- [18] Zhisong Fu, Bryan B. Thompson, and Michael Personick. 2014. MapGraph: A High Level API for Fast Development of High Performance Graph Analytics on GPUs. In *GRADES*. 2:1–2:6.
- [19] Bernard A. Galler and Michael J. Fischer. 1964. An improved equivalence algorithm. *Commun. ACM* 7, 5 (1964), 301–303.
- [20] Wentian Guo, Yuchen Li, Mo Sha, and Kian-Lee Tan. 2017. Parallel Personalized Pagerank on Dynamic Graphs. *PVLDB* 11, 1 (2017), 93–106.
- [21] Zhihao Jia, Yongkee Kwon, Galen M. Shipman, Patrick S. McCormick, Mattan Erez, and Alex Aiken. 2017. A Distributed Multi-GPU System for Fast Graph Processing. *PVLDB* 11, 3 (2017), 297–310.
- [22] Krzysztof Kaczmarski, Piotr Przyimus, and Paweł Rządewski. 2014. Improving High-Performance GPU Graph Traversal with Compression. In *ADBIS*. 201–214.
- [23] U. Kang and Christos Faloutsos. 2011. Beyond 'Caveman Communities': Hubs and Spokes for Graph Compression and Mining. In *ICDM*. 300–309.
- [24] Chinmay Karande, Kumar Chellapilla, and Reid Andersen. 2009. Speeding Up Algorithms on Compressed Web Graphs. *Internet Mathematics* 6, 3 (2009), 373–398.
- [25] Farzad Khorasani, Keval Vora, Rajiv Gupta, and Laxmi N. Bhuyan. 2014. CuSha: vertex-centric graph processing on GPUs. In *HPDC*. 239–252.
- [26] Min-Soo Kim, Kyuhyeon An, Himchan Park, Hyunseok Seo, and Jinwook Kim. 2016. GTS: A Fast and Scalable Graph Processing Method based on Streaming Topology to GPUs. In *SIGMOD*. 447–461.
- [27] Haewoon Kwak, Changhyun Lee, Hosung Park, and Sue B. Moon. 2010. What is Twitter, a social network or a news media?. In *WWW*. 591–600.
- [28] N. Jesper Larsson and Alistair Moffat. 1999. Offline Dictionary-Based Compression. In *DCC*. 296–305.
- [29] Xiaojie Lin, Rui Zhang, Zeyi Wen, Hongzhi Wang, and Jianzhong Qi. 2014. Efficient Subgraph Matching Using GPUs. In *ADC*. 74–85.
- [30] Hang Liu, H. Howie Huang, and Yang Hu. 2016. iBFS: Concurrent Breadth-First Search on GPUs. In *SIGMOD*. 403–416.
- [31] Sebastian Maneth and Fabian Peternek. 2015. A Survey on Methods and Systems for Graph Compression. *CoRR* abs/1504.00616 (2015).
- [32] Enrico Mastrostefano and Massimo Bernaschi. 2013. Efficient breadth first search on multi-GPU systems. *J. Parallel Distrib. Comput.* 73, 9 (2013), 1292–1305.
- [33] Duane Merrill, Michael Garland, and Andrew S. Grimshaw. 2015. High-Performance and Scalable GPU Graph Traversal. *ACM Trans. Parallel Comput.* 1, 2 (2015), 14–30.
- [34] NVIDIA. 2018. GPU-accelerated Libraries for Computing. <https://developer.nvidia.com/gpu-accelerated-libraries/>. Accessed: 2018-10-20.
- [35] Yuechao Pan, Yangzihao Wang, Yuduo Wu, Carl Yang, and John D. Owens. 2017. Multi-GPU Graph Analytics. In *IPDPS*. 479–490.
- [36] Amitabha Roy, Ivo Mihailovic, and Willy Zwaenepoel. 2013. X-Stream: edge-centric graph processing using streaming partitions. In *SOSP*. 472–488.
- [37] Arnon Rungswang and Bundit Manaskasemsak. 2012. Fast PageRank Computation on a GPU Cluster. In *PDP*. 450–456.
- [38] Mo Sha, Yuchen Li, Bingsheng He, and Kian-Lee Tan. 2017. Accelerating Dynamic Graph Analytics on GPUs. *PVLDB* 11, 1 (2017), 107–120.
- [39] Koichi Shirahata, Hitoshi Sato, and Satoshi Matsuoka. 2014. Out-of-core GPU memory management for MapReduce-based large-scale graph processing. In *CLUSTER*. 221–229.
- [40] Julian Shun and Guy E. Blelloch. 2013. Ligra: a lightweight graph processing framework for shared memory. In *PPoPP*. 135–146.
- [41] Julian Shun, Laxman Dhulipala, and Guy E. Blelloch. 2015. Smaller and Faster: Parallel Processing of Compressed Graphs with Ligra+. In *DCC*. 403–412.
- [42] Jyothish Soman, Kishore Kothapalli, and P. J. Narayanan. 2010. A fast GPU algorithm for graph connectivity. In *IPDPS Workshops*. 1–8.
- [43] Jyothish Soman and Ankur Narang. 2011. Fast Community Detection Algorithm with GPUs and Multicore Architectures. In *IPDPS*. 568–579.
- [44] Anuroop Sriram, Kollu Gautham, Kishore Kothapalli, P. J. Narayan, and R. Govindarajulu. 2009. Evaluating Centrality Metrics in Real-World Networks on GPU. (2009).
- [45] John A Stratton, Nasser Anssari, Christopher Rodrigues, I-Jui Sung, Nady Obeid, Liwen Chang, Geng Daniel Liu, and Wen-mei Hwu. 2012. Optimization and architecture effects on GPU computing workload performance. In *InPar*. 1–10.
- [46] Koji Ueno and Toyotaro Suzumura. 2013. Parallel distributed breadth first search on GPU. In *HiPC*. 314–323.
- [47] Yangzihao Wang, Yuechao Pan, Andrew A. Davidson, Yuduo Wu, Carl Yang, Leyuan Wang, Muhammad Osama, Chenshan Yuan, Weitang Liu, Andy T. Riffel, and John D. Owens. 2017. Gunrock: GPU Graph Analytics. *ACM Trans. Parallel Comput.* 4, 1 (2017), 3:1–3:49.
- [48] Hao Wei, Jeffrey Xu Yu, Can Lu, and Xuemin Lin. 2016. Speedup Graph Processing by Graph Ordering. In *SIGMOD*. 1813–1828.
- [49] Tianji Wu, Bo Wang, Yi Shan, Feng Yan, Yu Wang, and Ningyi Xu. 2010. Efficient PageRank and SpMV Computation on AMD GPUs. In *ICPP*. 81–89.
- [50] Xintian Yang, Srinivasan Parthasarathy, and P. Sadayappan. 2011. Fast Sparse Matrix-Vector Multiplication on GPUs: Implications for Graph Mining. *PVLDB* 4, 4 (2011), 231–242.
- [51] Jianlong Zhong and Bingsheng He. 2014. Medusa: Simplified Graph Processing on GPUs. *IEEE Trans. Parallel Distrib. Syst.* 25, 6 (2014), 1543–1552.

APPENDICES

A GPU'S ARCHITECTURE

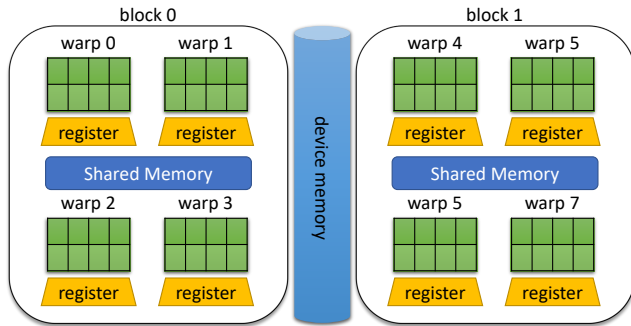


Figure 10: A sketch of GPU's architecture.

The superior performance achieved on GPUs in many computational applications mainly comes from GPU's two characteristics: (i) **Large Number of Cores**: A GPU die typically contains thousands of cores. Compared with CPUs, GPUs focus on numeric computation and hence, have a relatively simplified instruction set and manage to simplify the controlling logic in order to improve the theoretical computational performance. (ii) **High Memory Bandwidth**: Compared with CPUs, GPUs have a much higher memory bandwidth, up to hundreds of Gigabyte (GB) per second. In Figure 10, we illustrate GPU's computational architecture¹⁰. Warp is the smallest logic control unit on GPUs, and it is composed of a set of threads (generally 32 threads). The threads belonging to the same warp runs in the SIMT mode (i.e., single instruction multiple threads), and can achieve the fastest inter-thread communication through accessing each other's registers. Multiple warps compose a block (also known as CTA), which is the synchronization logic unit - only the threads belonging to the same block can conduct thread synchronization operations, and the cross-block threads cannot. Each block has its independent shared memory, so that the threads in the same block can communicate with each other efficiently. The shared memory and L1 cache have similar latency. Finally, a GPU card, as a complete subsystem, has its own memory unit called device memory. The memory bandwidth of a GPU card accessing its device memory can achieve hundreds of GB per second. However, if the data communication between CPU and GPU is needed, the device memory bandwidth will rely on PCIe transfer, which is typically below 16GB per second.

The threads in the same warp are synchronized in nature. Moreover, if multiple threads of the same warp enter into different condition branches (e.g., if-else), then all condition branches will be executed in a serial manner and the thread which enters the condition branch it does not belong to will

¹⁰This work is based on the CUDA architecture from NVIDIA and different versions of the CUDA architectures have some difference in between.

be idle. This is called “warp divergence”, and is a key consideration when evaluating the performance of GPU programs. From another perspective, GPU's high device memory access bandwidth comes from its relatively long cache line (L1 cache line is generally 128-byte, i.e., 32 single-precision variables). This means that if the memory access behaviors of all threads in the warp are aligned, they can achieve high device memory access bandwidth and thus, can accelerate the computation to a large extent. Otherwise, if such memory access behaviors are not aligned, a large amount of memory bandwidth will be wasted (no matter if it is needed or not, the data will be loaded into cache in 128-byte). This is called “uncoalesced memory access”, which is another key consideration when evaluating the performance of GPU programs.

Table 3: Examples of γ -code and ζ -code (bold digits indicate unary-code part)

integer	γ -code	ζ_2 -code	ζ_3 -code
1	1	101	1001
2	010	110	1010
3	011	111	1011
4	00100	010100	1100
5	00101	010101	1101
6	00110	010110	1110
12	0001100	011100	01001100
34	00000100010	001100010	01100010

B DETAILS ON VLC ENCODING

Most commonly used encoding schemes for applying VLC to compress graphs are γ -code [16] and ζ -code [8]. Both encoding schemes share some similar properties: they are specific to encoding positive integers, and have two parts in the encoding. The first half of γ -code uses unary-code¹¹ to represent the length of the element's significant bits, and the second half denotes the element's significant bits in binary representation. ζ -code is an extension of γ -code, which introduces a parameter k . If the value of the unary-code part in ζ_k -code encoding scheme is x , then it means that this element's length of significant bits is $k \times x$ in binary representation. Therefore, ζ_1 -code is equivalent to γ -code theoretically. In Table 3, we illustrate some examples in both the γ -code encoding scheme and the ζ_k -code encoding scheme. It should be noted that for γ -code, the preceding “1” in the second half can be omitted because it always starts with “1”. However, for ζ_k -code ($k \geq 2$), this does not hold. For instance, when encoding the number “6”, whose binary representation is “110”. In γ -code, we use the unary-code “001” to denote its length of significant bits is 3, followed by “10” as the significant bits after omitting the preceding “1”. In ζ_2 -code and ζ_3 -code, we use the unary-code “01” and “1” to represent the

¹¹https://en.wikipedia.org/wiki/Unary_coding

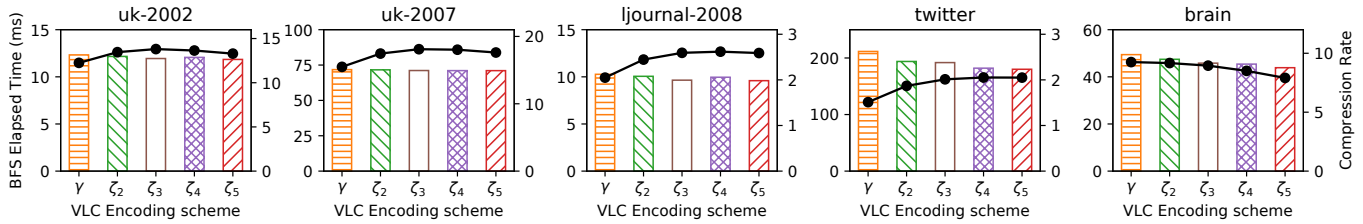


Figure 11: Results of varying VLC encoding schemes.

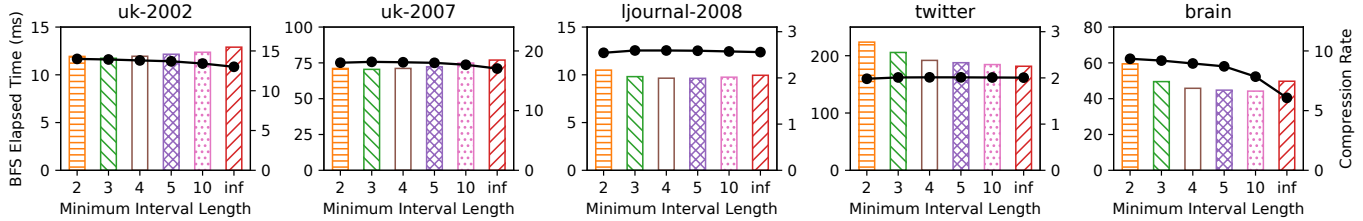


Figure 12: Results of varying Minimum Interval Lengths.

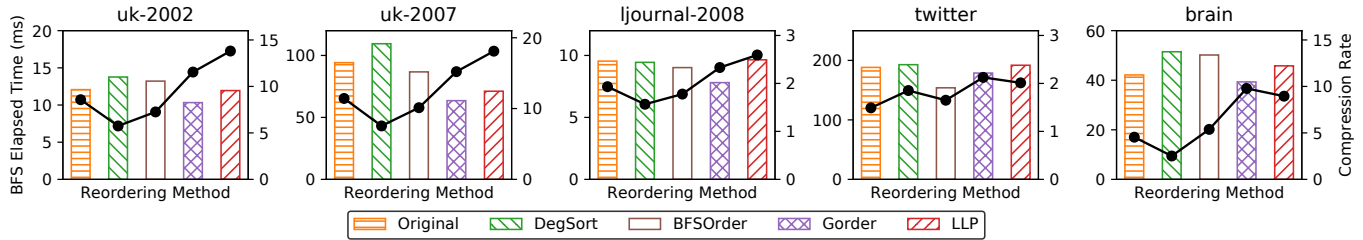


Figure 13: Results of varying Node Reordering Methods.

length of significant bits as 4 (2×2) and 3 (1×3), followed by “0110” and “110” as significant bits respectively.

C DETAILS ON CGR ENCODING

There are some implementation details on CGR encoding in order to achieve higher compression rate as follows.

- The gap value between the first interval’s starting node index or the first residual and the node whose neighbors are to be encoded can be negative, so a sign bit needs to be appended to the encoding. In particular, for the first encoding of both the first interval’s starting node index and the first residual, assume it is equal to x , then $2x$ is encoded if x is non-negative, otherwise, $2x + 1$ is encoded.
- The gap value is at least 1, and the interval length is no less than the minimum interval length. Therefore, we can shift the theoretical minimum to 0 in encoding in order to increase the compression rate.
- The VLC used in this work cannot represent 0 actually, so we conduct “+1” shifting for all encodings.

D PARAMETER SENSITIVITY ANALYSIS

In this subsection, we examine the influence of various parameters which are shown in Table 2.

VLC Encoding Scheme. Figure 11 shows the influence of different VLC encoding schemes with different k settings

(described in Appendix B) on both the computational latency and the compression rate. Varying k settings in VLC encoding schemes can pose an effect on the distribution of needed bit numbers of the encoding value range. Therefore, the tuning of k depends on the distribution of the concrete graph data structures. At the same time, instead of directly encoding the adjacency lists, CGR introduces mechanisms like Intervals and Residuals Representation, and Gap Transformation, which render the modelling of optimizing k more complicated. In [8], a simplified model is proposed which establishes a connection between the optimization of k and the exponent α in the power-law distribution¹². Theoretically, the workload is equal among decoding different VLC encoding schemes, and the varying of computational latency is mainly related to memory usage.

Minimum Interval Length. Figure 12 illustrates the effects of minimum interval length on the compression performance. This parameter indicates the minimum length of consecutive neighbors which can compose an interval and “inf” representing no interval. As for the compression rate, all settings of minimum interval length (except in brain) perform quite similarly, which means that brain highly benefits from the *Interval Representation* mechanism. A small minimum interval length leads to a large number of fragmented intervals and thus, degrades the computational efficiency.

¹²<https://en.wikipedia.org/wiki/Power-law>

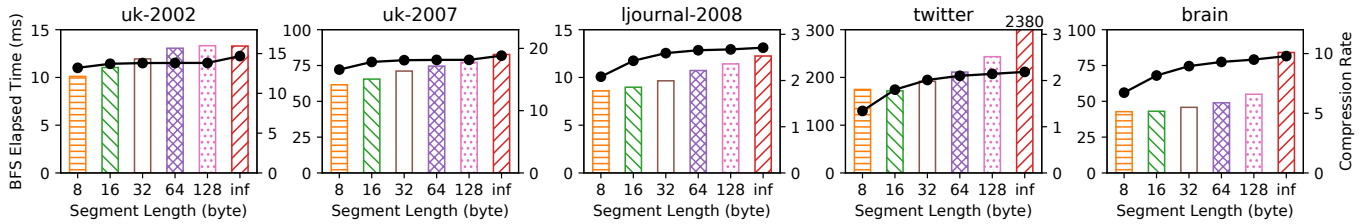


Figure 14: Results of varying Residual Segment Lengths.

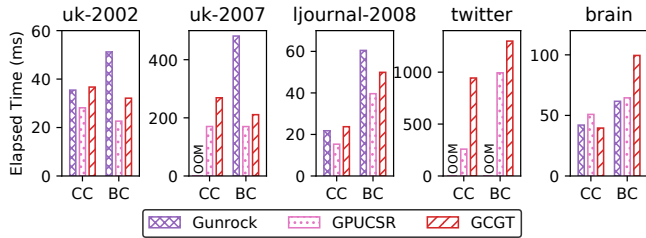


Figure 15: Experimental results of CC and BC.

This issue is more severe in twitter and brain, due to the existence of super nodes with too many neighbors for the former dataset, and relatively larger average out-degrees for the latter dataset. In the meanwhile, low compression rate of brain with no interval representation leads to high memory accesses, which obviously increases the elapsed time.

Node Reordering Methods. We choose several node reordering methods as follows in order to improve the locality of the original graphs.

- Original. The original order of the raw datasets.
- DegSort. The order provided by a straightforward greedy strategy, which sorts nodes in a descending order according to the frequencies that they are an out-degree node.
- BFSOrder [1]. The order generated by the breadth-first search traversal.
- Gorder [48]. The order is given based on a defined locality score **Gscore**, which is maximized by greedy strategies and partial maxTSP calculation on sliding windows.
- LLP [5]. The order is determined by the traversal among these clusters, which are distinguished by the layered label propagation algorithm.

We illustrate the influence of different node reordering methods in Figure 13. We first confirm that node reordering methods affect the compression rate in all datasets. Among these node reordering methods, LLP and Gorder perform significantly better than the intuitive strategies DegSort and BFSOrder to a large extent, due to their explicit optimization of the locality in the processing of reordering. Comparing LLP and Gorder, they are competitive. Across the datasets, LLP achieves higher compression rates and Gorder leads to faster computation. This is because the objective functions of LLP and Gorder are different: Gorder tends to generate dense

neighbor clusters for better cache performance whereas LLP optimizes towards global compression rate.

Residual Segment Length. We demonstrate the influence of various residual segment length settings in Figure 14. Residual segment length is a parameter to directly trade off computational latency for compression rate. A smaller residual segment length will generate more segments so that more threads can participate in the parallel processing. Nonetheless, at the same time, a larger blank area in the rear of each segment will be formed and this will harm the compression rate.

E EXPERIMENTAL RESULTS OF GCGT EXTENSIONS TO CC AND BC

We compare GCGT extensions to CC and BC with GPU-based baselines, Gunrock and GPUCSR, as illustrated in Figure 15. We run each program 100 times to calculate the average elapsed time and BC’s starting node is randomly selected. It can be verified that, compared with Gunrock and GPUCSR, GCGT extensions to CC and BC can achieve satisfactory performance, when operating CGR directly in the device memory.

As for CC, it links components via edge traversal which favors edge-centric implementations. Comparing GCGT and GPUCSR (J. Soman et al. [42], an edge-centric implementation), we find that in twitter, GCGT introduces relatively high overhead in terms of elapsed time, which is caused by the existence of super nodes (with large out-degrees). When utilizing edge frontiers, such characteristic is not a big problem, because after being added to a connected component, subsets of super nodes’ edges can be filtered out gradually and will not enter subsequent iterations. Nonetheless, this is not the same case when utilizing node frontiers. As a consequence, the computation of CC in twitter is not friendly to node-centric implementations.

As for BC, it is quite similar to BFS: deriving the σ -value and the δ -value through two BFS-like traversals. Thus, GCGT extension to BC exhibits similar performance as in BFS.

In summary, on the premise of incurring moderate cost, GCGT extensions to other graph applications can work directly on compressed graphs in order to effectively facilitate the device memory utilization.